

# To the Efficiency of a Green's Function Modification of the Method of Functional Equations

Yuri A Melnikov\*

Middle Tennessee State University, Murfreesboro, TN 37132, USA

## Abstract

Analysis of the computational potential is provided for a modification of one of the numerical approaches to the classical boundary integral equations method. The originally proposed name of the approach is the method of functional equations, but in nowadays it is also referred to as the fundamental solutions method. Undesired after effects of this name flip are pointed out. The modification, implemented in this study, requires computer-friendly representations for some relevant Green's function and significantly enhances the resolving potential of the method. This work focuses on the exploration of the computational applicability of this modification. Chosen for that boundary-value problems and stated on regions of irregular configuration for second order elliptic equations with discontinuous coefficients.

**Keywords:** Equations with discontinuous coefficients; Method of functional equations

## Introduction

This presentation aims at the analysis of computational potential of a modification of a well-known numerical approach to partial differential equations. The approach is based on the classical boundary integral equations method [1]. But prior to the analysis, we will attempt to restore a historical justice as to the title of that approach. Our viewpoint is presented on how the computational community had, with no reason, departed in 1985 from the original name of the method of functional equations proposed in [2] in 1964, and started calling it the fundamental solutions method. This created a confusing and distractive situation where two distinct names are linked to a single method. The departure from the original name had been undertaken in [3]. And what strikes the most is that the newly introduced name is irrelevant to the nature of the method. Yes, the fundamental solution concept is important for the method, but it is also vital for every of a wide spectrum of the numerical approaches developed in the boundary integral equations method. Hence, the term fundamental solution does not make the newly introduced name either clearly informative or uniquely distinguishable. A different feature makes in fact this method uniquely recognizable. Namely, this and only this method reduce a problem under consideration to functional equations. Just this very feature had motivated the method's creators Kupradze and Aleksidze when they came up in [2] with the original well-balanced name the method of functional equations. The name-flip in [3] was made quietly, without discussion. To trace out how that happened, recall the title of [2] "The method of functional equations for the approximate solution of certain boundary-value problems" and then read how the author of [3] cites that paper: "Usually related to the boundary integral equations method is the fundamental solutions method." Following [3], a misled part of the computational community had begun to refer to the method with the newly introduced name. So, the damage to justice was made. The name-flip generated an ill-posed opinion that the last publication on the method of functional equations is dated nearly fifty years ago, whereas the fundamental solutions method has been widely used through all these years. The opinion is senseless, but its very existence is hard unfortunately to ignore. Our long time [4,5-8] involvement with the boundary integral equation method reveals high computational potential of a specific modification of the method

of functional equations, which we originally proposed in [4]. The modification utilizes some Green's functions relevant to the considered problem, and will be called herein the Green's function modification of the method of functional equations (abbreviated as GF-MFE). The GF-MFE represents a semi-analytical technique. At its analytical stage, a special integral representation is constructed for the solution of the considered boundary-value problem, with an appropriate Green's function (being referred to, in this study, as the resolving Green's function) used for the kernel of that integral representation. Note that it is absolutely critical to possess a computer-friendly resolving Green's function. The numerical stage of the GF-MFE is, in turn, based on a more or less traditional meshless numerical scheme. An important feature of the GF-MFE predetermines its computational effectiveness, making it especially attractive for users. Due to properties of resolving Green's functions, some of the boundary conditions in the considered problem are satisfied prior to a numerical work. This implies that the resultant functional equations do not require a numerical solution over the entire boundary of the region, notably enhancing the practicality of the GF-MFE. The computational potential of the GF-MFE is targeted in this study. The method will be applied to boundary-value problems stated on regions of irregular configuration for equations whose coefficients are not necessarily continuous functions. We focus on the construction of computer-friendly representations of Green's functions for such problems.

## Description of the GF-MFE procedure

Let a two-dimensional multiply-connected region  $\Omega_0$  be bounded with a piecewise smooth contour  $\tau = U_{j=0}^m \tau_j$ , where the exterior contour  $\Gamma_0$  is either closed or semi-closed, whilst  $\tau_j, (j = \overline{1, m})$  represent closed interior contours that do not overlap with each other.  $\Omega_0$  could

\*Corresponding author: Yuri A Melnikov, Middle Tennessee State University, Murfreesboro, TN 37132, USA, Tel: 1-615-898-2300; E-mail: [Yuri.Melnikov@mtsu.edu](mailto:Yuri.Melnikov@mtsu.edu)

Received February 24, 2014; Accepted April 17, 2014; Published April 25, 2014

Citation: Melnikov YA (2014) To the Efficiency of a Green's Function Modification of the Method of Functional Equations. J Appl Computat Math 3: 162 doi:10.4172/2168-9679.1000162

Copyright: © 2014 Melnikov YA. This is an open-access article distributed under the terms of the Creative Commons Attribution License, which permits unrestricted use, distribution, and reproduction in any medium, provided the original author and source are credited.

also be interpreted as the simply-connected region  $\widetilde{\Omega}_0$  bounded with  $\Gamma_0$  and weakened with  $m$  apertures whose contours are  $\Gamma_j$ . In  $\Omega_0$ , we consider a well-posed linear homogeneous boundary-value problem

$$L_0[w_0(P)] = 0, P \in \Omega_0 \quad (1)$$

$$B_0[w_0(P)] = 0, P \in \Gamma_0 \quad (2)$$

$$B_j[w_j(P)] = 0, P \in \Gamma_j, j = \overline{1, m} \quad (3)$$

allowing only the trivial solution  $w(P)=0$ . Here  $L$  represents a second order linear differential operator with possibly piecewise constant coefficients, whilst  $B_0$  and  $B_j$  are linear first order operators imposing one of the three standard types of boundary conditions of either Dirichlet, or Neumann, or Robin type, with a single one of these conditions being imposed on each of the interior contours. As to a physical process or phenomenon that could be simulated with the above problem statement, one might recall, for example, a two-dimensional steady-state diffusion type process in a thin plate made of a piecewise homogeneous conductive material, with the plate's middle plane occupying the region  $\Omega_0$ . The focus in this study is, in part, on the analysis of the computational potential of a semi-analytical approach implemented to the construction of the Green's function  $G(P, Q)$  to the boundary-value problem in (1)-(3). To describe the approach in necessary detail, let  $\widetilde{G}(P, Q)$  represent the Green's function of the boundary-value problem stated in (1) and (2) on the simply connected region  $\widetilde{\Omega}_0$ . To avoid a confusion of dealing with the two Green's functions,  $\widetilde{G}(P, Q)$  will be referred to, in what follows, as the resolving Green's function. The latter is supposed to be available prior to a numerical treatment of the problem in (1)-(3). Proceeding with the approach, originally proposed in [4], we express the Green's function  $G(P, Q)$  of the boundary-value problem of (1)-(3) in terms of the resolving function  $\widetilde{G}(P, Q)$  as

$$G(P, Q) = \widetilde{G}(P, Q) + U_Q(P), \quad (4)$$

where the second term represents an additive component to the regular term of the Green's function  $G(P, Q)$  that we are looking for. Evidently, for the source point  $Q^*$  arbitrarily fixed in  $\Omega_0$ , the component  $U_{Q^*}(P)$  must represent the solution to the boundary-value problem

$$L[U_{Q^*}(P)] = 0, P \in \Omega_0 \quad (5)$$

$$B_0[U_{Q^*}(P)] = 0, P \in \Gamma_0 \quad (6)$$

$$B_j[U_{Q^*}(P)] = \varphi_j(P), P \in \Gamma_j, j = \overline{1, m} \quad (7)$$

with  $\varphi_j(P)$  being the traces that the operators  $B_j$ , acting on  $\widetilde{G}(P, Q^*)$ , leave on  $\Gamma_j$ . That is,  $\varphi_j(P) = B_j[\widetilde{G}(P, Q^*)], P \in \Gamma_j, j = \overline{1, m}$

From the representation in (4), it follows that, since the function  $U_{Q^*}(P)$  is assumed to be regular everywhere in  $\Omega_0$  (at  $P=Q^*$ , in particular), the Green's function  $G(P, Q)$  possesses the same type of principal singularity as  $\widetilde{G}(P, Q)$ .

Taking advantage of the defining properties of  $\widetilde{G}(P, Q)$ , it sounds reasonable to express the solution  $U_Q(P)$  to the problem in (5) - (7) in the integral form

$$U_{Q^*}(P) = \sum_{j=1}^m \int_{\Gamma_j} \widetilde{G}(P, S) \mu_j(S) d\Gamma_j'(S), P \in \Omega_0 \quad (8)$$

where  $\Gamma_j'$ , ( $j = \overline{1, m}$ ) represent some closed piecewise-smooth lines (which will be referred to, in this presentation, as the fictitious contours),

each of which is located: (i) entirely inside of the corresponding aperture contour  $\Gamma_j$  and (ii) reasonably close to the latter. The density functions  $\mu_j(Q)$  in (8) are assumed integrable on  $\Gamma_j'$ . It is evident that, due to the defining properties of the resolving Green's function, on one hand, and to the fact that the fictitious contours are located outside of  $\Omega_0$ , on the other hand, the representation in (8) satisfies the governing differential equation in (5) everywhere in  $\Omega_0$ . Moreover, the boundary condition in (6) is also satisfied, regardless of the density functions  $\mu_j(Q)$ . Thus, the presence of the latter provides the representation in (8) with some degree of freedom, which can be used to satisfy the boundary conditions in (7). Taking the field point  $P$  in (8) to the factual aperture contours  $\Gamma_j$ ; ( $j = \overline{1, m}$ ), we obtain an  $m \times m$  system of regular functional equations in the density functions  $\mu_j(S)$ . The system appears in form

$$-\varphi_i(P) = \sum_{j=1}^m \int_{\Gamma_j} \widetilde{G}(P, S) \mu_j(S) d\Gamma_j'(S), P \in \Gamma_i, i = \overline{1, m} \quad (9)$$

Two comments are offered as to the classification of the above system. First, its regularity is supported by the fact that each  $\Gamma_j'$ , hosting the source point  $S$  in the integral representation of (8), has no common points with the corresponding actual aperture contour  $\Gamma_j$ , which represents the domain for the coordinates of the observation point  $P$  in (8). Thus, the kernel function  $\widetilde{G}(P, S)$  in (9) is regular indeed. The second important comment with regard to (9) relates to the term functional. Due to the presence of integral operators, it sounds reasonable to call the system integral. But the use of this term could not be formally justified, because in a classical integral equation, both the variables  $P$  and  $Q$  belong to the same domain. But this is not the case for (9). That is why the term functional equations of integral type are perhaps the best fit for the equations in (9). Clearly, the proposed approach represents a regularizing procedure for the Green's function version of the standard boundary integral equation method, parameters. Optimal values of those can be found through a numerical experiment for each particular problem individually. Our focus will also be on another class of problems, that involves the geometry as in the setting of (1)-(3), but deals, however, with a different physics. Providing specifics let the multiply-connected region  $\Gamma_0$  be bounded with a piecewise-smooth outer contour  $\Gamma_0$  and smooth inner contours  $\Gamma_j$ , ( $j = \overline{1, m}$ ). Let also  $\Omega_0$  be filled with a material whose conductive property is specified by a piecewise constant function  $\lambda_0(P)$ . Let, in addition, each aperture  $\Omega_j$ , ( $j = \overline{1, m}$ ) in  $\Omega_0$  is filled with a foreign homogeneous isotropic material whose conductivity is  $\lambda_j$ . This gives rise to the boundary-value problem

$$L_0[w_0(P)] = 0, P \in \Omega_0 \quad (10)$$

$$B_0[w_0(P)] = 0, P \in \Gamma_0 \quad (11)$$

$$L_j[w_j(P)] = 0, P \in \Omega_j, j = \overline{1, m} \quad (12)$$

$$w_0(P) = w_j(P), P \in T_j, j = \overline{1, m} \quad (13)$$

$$\frac{\partial w_0(P)}{\partial n_j} = \Lambda_j \frac{\partial w_j(P)}{\partial n_j}, P \in T_j, j = \overline{1, m} \quad (14)$$

in  $w_j(P)$ , ( $j = \overline{0, m}$ ), stated in the piecewise homogeneous region  $\Omega = \bigcap_{j=0}^m \Omega_j$ . Here  $L_0$  and  $L_j$  represent linear second order elliptic operators,  $B_0$  is a linear first order operator of a boundary condition imposed on  $\Gamma_0$ , the factors  $\Lambda_j$  in (14) are defined as  $\Lambda_j = \lambda_j / \lambda_0(P)$ , and  $n_j$  are the outward normal to  $\Gamma_j$ . Since the coefficients in (10) and (12) are not differentiable in  $\Omega$ , the classical Green's function approach does not apply to a problem setting of the kind in (10)-(14). We turn therefore to the extension of the Green's function formalism proposed

in [5]. It gives rise to the concept of matrix of Green's type.

A semi-analytical procedure proposed for the construction of such a matrix

$$G(P, Q) = (G_{ij}(P, Q))_{i,j=0,m}$$

for the boundary-value problem stated in (10)-(14) will be described below. But prior to that, we highlight a specific feature of  $G(P, Q)$  with regard to the location of  $P$  and  $Q$ . Note that, in the  $ij$ -th element  $G_{ij}(P, Q)$  of  $G(P, Q)$ ,  $P$  and  $Q$  are located in different fragments of  $\Omega$ . Namely,  $P$  belongs to  $\Omega_i$ , whilst  $Q \in \Omega_j$ . So, in the peripheral elements  $G_{0j}(P, Q)$ , of the first row of  $G(P, Q)$ , for example, the observation point is located in  $\Omega_0$ , while the corresponding inclusion  $\Omega_j$  hosts the source point. Consequently,  $P$  might coincide with  $Q$  only in the main diagonal elements  $G_{ii}(P, Q)$  of  $G(P, Q)$ , implying that those elements possess the principal singularity related to the fundamental solutions of (10) and (12). Whereas, the peripheral elements  $G_{ij}(P, Q)$  are regular functions.

To illustrate the essentials of our approach, we consider the steady-state heat conduction in the half-plane  $\Omega = \{y > 0\}$  filled with an isotropic homogeneous material ( $\lambda_0$ ) and containing an inclusion  $\Omega_1$ , made of another isotropic homogeneous material ( $\lambda_1$ ). The ideal thermal contact is assumed on  $\Gamma_1$ , and the Dirichlet condition is imposed on  $y=0$ . This yield

$$\frac{\partial^2 u_0(x, y)}{\partial x^2} + \frac{\partial^2 u_0(x, y)}{\partial y^2} = 0, (x, y) \in \Omega_0 = \Omega \setminus \Omega_1, \quad (15)$$

$$\frac{\partial^2 u_1(x, y)}{\partial x^2} + \frac{\partial^2 u_1(x, y)}{\partial y^2} = 0, (x, y) \in \Omega_1, \quad (16)$$

$$u_0(x, 0) = 0, \lim_{\delta x \rightarrow \pm 0} u_0(x, y) < \infty \quad (17)$$

and

$$u_0(x, y) = u_1(x, y), \frac{\partial u_0(x, y)}{\partial n} = \lambda \frac{\partial u_1(x, y)}{\partial n}, (x, y) \in \Gamma_1 \quad (18)$$

on the half-plane with the inclusion, where  $\lambda = \lambda_1 = \lambda_0$  and

$$\frac{\partial}{\partial n} \equiv c \cos(\widehat{n, x}) \frac{\partial}{\partial n} \wedge + \cos(\widehat{n, y}) \frac{\partial}{\partial y}$$

Applying the definition introduced in [5] to the matrix of Green's type  $G(x, y; \xi, \eta) = (G_{ij}(x, y; \xi, \eta))_{i,j=0,1}$  of the problem in (15)-(18), we identify the entry  $G_{ij}(x, y; \xi, \eta)$  of  $G(x, y; \xi, \eta)$  with the potential field, which is generated in  $\Omega_j$  ( $i=0,1$ ) by a point source located in  $\Omega_j$  ( $j=0,1$ ). The main-diagonal elements of  $G(x, y; \xi, \eta)$  must possess the logarithmic singularity, whereas  $G_{01}(x, y; \xi, \eta)$  and  $G_{10}(x, y; \xi, \eta)$  are, as functions of  $x$  and  $y$ , just harmonic everywhere in  $\Omega_0$  and  $\Omega_1$ , respectively. We look for  $G_{00}(x, y; \xi^*, \eta^*)$  with  $\xi^*, \eta^*$  arbitrarily fixed in  $\Omega_0$ , in the form

$$G_{00}(x, y; \xi^*, \eta^*) = \widehat{G}(x, y; \xi^*, \eta^*) + g_{00}^*(x, y), (x, y) \in \Omega_0 \quad (19)$$

where  $\widehat{G}(x, y; \xi^*, \eta^*)$  is the classical [9,10] Green's function of the Dirichlet problem for the half-plane  $\{y > 0\}$ , which brings the required logarithmic singularity to  $G_{00}(x, y; \xi^*, \eta^*)$  while the harmonic component  $g_{00}^*(x, y)$  can be found in a form of the modified potential

$$g_{00}^*(x, y) = \int_{F_{in}} \widehat{G}(x, y; \xi, \eta) \mu_{in}(\xi, \eta), (x, y) \in \Omega_0 \quad (20)$$

where  $F_{in}$  is a fictitious contour embraced by the interfacial line  $\Gamma_1$ . For  $G_{10}(x, y; \xi^*, \eta^*)$ , with  $\xi^*, \eta^* \in \Omega_0$ , we construct the potential

$$G_{10}(x, y; \xi^*, \eta^*) = \int_{F_{ex}} \phi(x, y; \xi, \eta) \mu_{ex}(\xi, \eta) dF_{ex}, (\xi, \eta), (x, y) \in \Omega_1 \quad (21)$$

where  $F_{ex}$  is a fictitious contour embracing  $\Gamma_1$ . The kernel  $\Phi(x, y; \xi, \eta)$  of the above representation is the fundamental solution [1] of the Laplace equation in two dimensions. This makes  $G_{10}(x, y; \xi^*, \eta^*)$  harmonic everywhere in  $\Omega_1$ .

The densities in  $\mu_{in}(\xi, \eta)$  and  $\mu_{ex}(\xi, \eta)$  in (20) and (21) can be found from the contact conditions in (18). The first of these yields

$$\begin{aligned} \widehat{G}(x, y; \xi^*, \eta^*) + \int_{F_{in}} \widehat{G}(x, y; \xi, \eta) \mu_{in}(\xi, \eta) dF_{in}, (\xi, \eta) \\ - \int_{F_{ex}} \phi(x, y; \xi, \eta) \mu_{ex}(\xi, \eta) dF_{ex}, (\xi, \eta) = 0, (x, y) \in \Gamma_1 \end{aligned} \quad (22)$$

whilst the second condition results in

$$\begin{aligned} \frac{\partial \widehat{G}(x, y; \xi^*, \eta^*)}{\partial n} + \int_{F_{in}} \frac{\partial \widehat{G}(x, y; \xi, \eta)}{\partial n} \mu_{in}(\xi, \eta) dF_{in}, (\xi, \eta) \\ = \lambda \int_{F_{ex}} \frac{\partial \phi(x, y; \xi, \eta)}{\partial n} \mu_{ex}(\xi, \eta) dF_{ex}, (\xi, \eta), (x, y) \in \Gamma_1 \end{aligned} \quad (23)$$

The relations in (22) and (23) represent a system of regular functional equations in  $\mu_{in}(\xi, \eta)$  and  $\mu_{ex}(\xi, \eta)$ , and can easily be solved numerically. Shape and location of the fictitious contours should be determined on the case-by-case basis.

So, pro les of the elements  $G_{00}(x, y; \xi^*, \eta^*)$  and  $G_{10}(x, y; \xi^*, \eta^*)$  can be computed once an approximate solution to the system in (22) and (23) is found, with the density functions  $\mu_{in}(\xi, \eta)$  and  $\mu_{ex}(\xi, \eta)$  substituted into (20) and (21). As to the other two entries  $G_{01}(x, y; \xi^*, \eta^*)$  and  $G_{11}(x, y; \xi^*, \eta^*)$  of  $G(x, y; \xi^*, \eta^*)$ , with the source point  $(\xi^*, \eta^*)$  arbitrarily fixed in  $\Omega_1$ , we express them as

$$G_{01}(x, y; \xi^*, \eta^*) = \int_{F_{in}} \widehat{G}(x, y; \xi, \eta) v_{in}(\xi, \eta) dF_{in}, (\xi, \eta), (x, y) \in \Omega_0$$

and

$$G_{11}(x, y; \xi^*, \eta^*) = \phi(x, y; \xi^*, \eta^*) + g_{11}^*(x, y) \in \Omega_1 \quad (24)$$

where

$$g_{11}^*(x, y) = \int_{F_{ex}} \phi(x, y; \xi, \eta) v_{ex}(\xi, \eta) dF_{ex}, (\xi, \eta), (x, y) \in \Omega_1 \quad (25)$$

The densities in  $v_{in}(\xi, \eta)$  and  $v_{ex}(\xi, \eta)$  of the potentials in (24) and (25) can also be found by virtue of the conditions in (18), which yield

$$\phi(x, y; \xi^*, \eta^*) + \int_{F_{in}} \phi(x, y; \xi, \eta) v_{ex}(\xi, \eta) dF_{ex}, (\xi, \eta) - \int_{F_{in}} \widehat{G}(x, y; \xi, \eta) v_{in}(\xi, \eta) dF_{in}, (\xi, \eta) = 0, (x, y) \in \Gamma_1$$

and

$$\frac{\partial \phi(x, y; \xi^*, \eta^*)}{\partial n} + \int_{F_{ex}} \frac{\partial \phi(x, y; \xi, \eta)}{\partial n} v_{ex}(\xi, \eta) dF_{ex}, (\xi, \eta) = \lambda \int_{F_{in}} \frac{\partial \widehat{G}(x, y; \xi, \eta)}{\partial n} v_{in}(\xi, \eta) dF_{in}, (\xi, \eta), (x, y) \in \Gamma_1$$

As soon as the above regular system is solved numerically, one can accurately compute profiles of  $G_{01}(x, y; \xi^*, \eta^*)$  and  $G_{11}(x, y; \xi^*, \eta^*)$  upon substituting the density functions  $v_{in}(\xi, \eta)$  and  $v_{ex}(\xi, \eta)$  into (24) and (25). The shape and location of  $F_{in}$  and  $F_{ex}$  ought to be found by a numerical experiment. In light of the superposition principle, we can consider the half-plane  $\Omega = \{y > 0\}$  containing an inclusion, if a finite number of sources of different intensities are located inside and outside of the inclusion.

Computational potential of the described algorithm will be explored in Numerical illustrations part, but prior to that a number of resolving

Green's functions  $\tilde{G}(P; Q)$ , representing an essential instrument of the algorithm, will be presented in what follows.

### Resolving Green's Functions

The classical Green's function of the Dirichlet problem for the Laplace equation on the half-plane  $y > 0$ , which was earlier employed in the Description of the GF-MFE procedure part as the resolving Green's function for the problem in (15)-(18), will be also used in Numerical illustrations.

In another problem setting in Numerical illustrations section, we obtain the Green's function for the Laplace equation posed on a double-connected region  $\Omega$  representing the semi-infinite strip  $\Omega_0 = \{Re(z) > 0, 0 < Im(z) < b\}$ , weakened with an aperture. Three standard types (Dirichlet, Neumann, and Robin) of boundary conditions

$$\left(\frac{\partial u}{\partial x} - \beta u\right)\Big|_{x=0} = 0, \beta \geq 0; u\Big|_{y=0} = 0, \frac{\partial u}{\partial y}\Big|_{y=b} = 0$$

are imposed on the outer boundary of  $\Omega$ . The representation

$$G(x, y; \xi, \eta) = \frac{1}{2\pi} \ln \left| \frac{1 - e^{\rho(z-\bar{\xi})}}{1 - e^{\rho(z+\bar{\xi})}} \right| + \frac{1}{2\pi} \ln \left| \frac{1 - e^{\rho(z-\xi)}}{1 - e^{\rho(z+\xi)}} \right| - \frac{2\beta}{b} \sum_{n=1}^{\infty} \frac{e^{-\nu(x+\xi)}}{\nu(\nu+\beta)} \sin \nu y \sin \nu \eta, \nu = (2n-1)\frac{\pi}{b}, p = \frac{\pi}{2b} \quad (26)$$

is implemented for the resolving Green's function in that case. The complex variable notations  $z = x + iy$  and  $\zeta = \xi + i\eta$  are used for compactness in (26). Its derivation can be found in [8]. To introduce another representation, which can potentially be used as the resolving Green's function in the GF-MFE, consider the semi-infinite  $\Omega = \{-a < x < \infty, 0 < y < b\}$  composed  $\Omega_1 = \{-a < x < 0, 0 < y < b\}$  and  $\Omega_2 = \{0 < x < \infty, 0 < y < b\}$  and pose the following boundary-value problem

$$\begin{aligned} \frac{\partial u_1(-a, y)}{\partial x} - \beta u_1(-a, y) &= 0, \beta \geq 0; \lim_{x \rightarrow \infty} |u_2(x, y)| < \infty \\ u_1(0, y) &= u_2(0, y), \frac{\partial u_1(0, y)}{\partial x} = \lambda \frac{\partial u_2(0, y)}{\partial x} \\ u_i(x, 0) &= \frac{\partial u_i(x, b)}{\partial y} = 0, i = 1, 2 \end{aligned} \quad (29)$$

for the static Klein-Gordon equations

$$\frac{\partial^2 u_i(x, y)}{\partial x^2} + \frac{\partial^2 u_i(x, y)}{\partial y^2} - k_i^2 u_i(x, y) = 0, (x, y) \in \Omega_i, i = 1, 2 \quad (30)$$

where the functions  $u_1(x, y)$  and  $u_2(x, y)$  are defined in  $\Omega_1$  and  $\Omega_2$ , respectively, and  $\lambda = \lambda_2 / \lambda_1$  stays for the relative material conductivity, with  $\lambda_1$  and  $\lambda_2$  representing the conductivities of materials  $\Omega_1$  and  $\Omega_2$ .

Following the extension of the Green's function formalism, we obtain the elements  $\tilde{G}(x, y; \xi, \eta)$  of the matrix of Green's type

$$\tilde{G}(x, y; \xi, \eta) = \left( \tilde{G}_{ij}(x, y; \xi, \eta) \right)_{i, j=1, 2}$$

for the problem setting in (27)-(30) in the form

$$\tilde{G}_{ij}(x, y; \xi, \eta) = \frac{2}{b} \sum_{n=1}^{\infty} \frac{g_{ij}^n(x, \xi)}{\Delta} \sin \nu y \sin \nu \eta, \frac{(2n-1)\pi}{2b} \quad (31)$$

Where  $\Delta = (h_1 + \lambda h_2)(h_1 + \beta) e^{2h_1 a} + (h_1 - \lambda h_2)(h_1 - \beta)$  and the

parameters  $h_i$  are defined as  $h_i = \sqrt{\nu^2 + k_i^2}$ , ( $i = 1, 2$ )

We just present the coefficient  $g_{11}^n(x, \xi)$  of

$$g_{11}^n(x, \xi) = \frac{1}{2h_1} \left\{ (h_1 + \beta) \left[ (h_1 + \lambda h_2) e^{-h_1|x-\xi|} + (h_1 - \lambda h_2) e^{h_1|x+\xi|} \right] e^{2h_1 a} + (h_1 - \beta) \left[ (h_1 + \lambda h_2) e^{h_1|x+\xi|} + (h_1 - \lambda h_2) e^{-h_1|x-\xi|} \right] \right\} \quad (31)$$

Note that a certain analytical effort is recommended as to the diagonal elements of  $\tilde{G}(x, y; \xi, \eta)$  possessing the logarithmic singularity.

To introduce another resolving Green's function, we consider the half-plane  $\Omega = \{0 < r < \infty, 0 < \varphi < \pi\}$  composed  $\Omega_1 = \{0 < r < \infty, 0 < \varphi < \pi\}$  and pose the problem

$$\frac{1}{r} \frac{\partial}{\partial r} \left( r \frac{\partial u_i(r, \varphi)}{\partial r} \right) + \frac{1}{r^2} \frac{\partial^2 u_i(r, \varphi)}{\partial \varphi^2} = 0, (r, \varphi) \in \Omega_i, i = 1, 2 \quad (32)$$

$$\lim_{r \rightarrow 0} |u_1(r, \varphi)| < \infty, \lim_{r \rightarrow 0} |u_2(r, \varphi)| < \infty \quad (33)$$

$$u_1(a, \varphi) = u_2(a, \varphi), \frac{\partial u_1(a, \varphi)}{\partial r} = \lambda \frac{\partial u_2(a, \varphi)}{\partial r} \quad (34)$$

$$u_i(r, 0) = u_2(r, 0), u_1(r, \pi) = u_2(r, \pi) = 0 \quad (35)$$

The closed analytical form

$$G_{11}(r, \varphi; \rho, \psi) = \frac{1}{4\pi} \left[ \ln \frac{r^2 - 2r\rho \cos(\varphi + \psi) + \rho^2}{r^2 - 2r\rho \cos(\varphi - \psi) + \rho^2} \right] - \frac{\lambda - 1}{\lambda + 1} \left[ \ln \frac{a^4 - 2a^2 r \rho \cos(\varphi + \psi) + r^2 \rho^2}{a^4 - 2a^2 r \rho \cos(\varphi - \psi) + r^2 \rho^2} \right] \quad (36)$$

$$\tilde{G}_{12}(r, \varphi; \rho, \psi) = \frac{\lambda}{2\lambda(\lambda + 1)} \ln \frac{r^2 - 2r\rho \cos(\varphi + \psi) + \rho^2}{r^2 - 2r\rho \cos(\varphi - \psi) + \rho^2} \sim \quad (37)$$

$$\tilde{G}_{21}(r, \varphi; \rho, \psi) = \frac{\lambda}{2\lambda(\lambda + 1)} \ln \frac{r^2 - 2r\rho \cos(\varphi + \psi) + \rho^2}{r^2 - 2r\rho \cos(\varphi - \psi) + \rho^2} \quad (38)$$

and

$$\tilde{G}_{22}(r, \varphi; \rho, \psi) = \frac{1}{4\lambda} \left[ \ln \frac{r^2 - 2r\rho \cos(\varphi + \psi) + \rho^2}{r^2 - 2r\rho \cos(\varphi - \psi) + \rho^2} \right] + \frac{\lambda - 1}{\lambda + 1} \ln \frac{a^4 - 2a^2 r \rho \cos(\varphi + \psi) + r^2 \rho^2}{a^4 - 2a^2 r \rho \cos(\varphi - \psi) + r^2 \rho^2} \quad (39)$$

of the elements of the matrix of Green's type (32)-(35) can be found in [6]. The matrix of Green's type  $\tilde{G}(r, \varphi; p, \psi)$  for the problem in  $\tilde{G}(x, y; \xi, \eta) = \left( \tilde{G}_{ij}(x, y; \xi, \eta) \right)_{i, j=1, 2}$  of the boundary-value problem

$$\frac{\partial^2 u_i(x, y)}{\partial x^2} + \frac{\partial^2 u_i(x, y)}{\partial y^2} = 0, (x, y) \in \Omega_i, i = 1, 2, 3 \quad (40)$$

$$\lim_{x \rightarrow \infty} |u_1(x, y)| < \infty, \lim_{x \rightarrow \infty} |u_3(x, y)| < \infty \quad (41)$$

$$u_1(-a, y) = u_2(-a, y), \lambda_1 \frac{\partial u_1(-a, y)}{\partial x} = \lambda_2 \frac{\partial u_2(-a, y)}{\partial x} \quad (42)$$

$$u_2(a, y) = u_3(a, y), \lambda_2 \frac{\partial u_2(a, y)}{\partial x} = \lambda_3 \frac{\partial u_3(a, y)}{\partial x} \quad (43)$$

$$u_i(x, 0) = \frac{\partial u_i(x, b)}{\partial y} = 0, i = 1, 2, 3 \quad (44)$$

can also be used as a resolving Green's function. The elements  $\tilde{G}_{ij}(x, y; \xi, \eta)$  of  $\tilde{G}(x, y; \xi, \eta)$  are obtained

$$\tilde{G}_{ij}(x, y; \xi, \eta) = \frac{1}{b} \sum_{n=1}^{\infty} \frac{g_{ij}^n(x, \xi)}{v \Delta^*} \sin v y \sin v \eta, v = \frac{(2n-1)\pi}{2b} \quad (45)$$

where  $\Delta^* = (1 + \Lambda_1)(1 + \Lambda_2)e^{4va} + (1 - \Lambda_1)(1 + \Lambda_2)$  with  $\Lambda_1 = \lambda_2 / \lambda_1$  and  $\Lambda_2 = \lambda_3 / \lambda_2$ .

The series coefficient  $g_{11}^n(x, \xi)$  for example, in (45) reads as

$$g_{11}^n(x, \xi) = \left[ (1 - \Lambda_1)(1 + \Lambda_2)e^{4va} + (1 + \Lambda_1)(1 - \Lambda_2) \right] e^{v(x+\xi+2a)} + \Delta^* e^{-v|x-\xi|}$$

The convergence rate of the series in (45) is low (1/n) for the diagonal elements. To enhance it, one can use the procedure proposed in [6] and [7]. This reduces the element to the computer-friendly form

$$\tilde{G}_{11}(x, y; \xi, \eta) = \frac{1}{2\pi} \left\{ \ln \left| \frac{1 + e^{p(z-\zeta)}}{1 - e^{p(z-\zeta)}} \right| \left| \frac{1 - e^{p(z-\bar{\zeta})}}{1 + e^{p(z-\bar{\zeta})}} \right| + \frac{(1 - \Lambda_1)}{(1 - \Lambda_2)} \ln \left| \frac{1 + e^{p(z+\zeta_1)}}{1 - e^{p(z+\zeta_1)}} \right| \left| \frac{1 - e^{p(z+\bar{\zeta}_1)}}{1 + e^{p(z+\bar{\zeta}_1)}} \right| \right. \\ \left. + \frac{16 \Lambda_1 (1 - \Lambda_2)}{(1 + \Lambda_1)} \sum_{n=1}^{\infty} \frac{e^{v(x+\xi+2a)}}{(2n-1)\Delta^*} \sin v y \sin v \eta \right\}$$

Where  $p = \pi/2b$ . Along with the complex variables  $z$  and  $\zeta$  we introduced the expressions  $z_1 = (x+a) + iy$ , and  $\zeta_1 = (\xi+a) + i\eta$ . The component  $\ln \left| \frac{1 + e^{p(z-\zeta)}}{1 - e^{p(z-\zeta)}} \right|$  in the above expression represents the singular part of  $\tilde{G}_{11}(x, y; \xi, \eta)$

### Numerical Illustrations

Specific computational features of our approach will be monitored. We plan, in particular, to figure out how the shape of apertures and inclusions affects the solution accuracy level attained. Our focus will also be on the proximity of apertures and inclusions to each other and to the contours of considered regions. In addition, we aim at the analysis of the algorithm as to the proximity of point sources to contours of either apertures or inclusions.

But before going to specifics, a sample problem is considered to estimate the accuracy level attainable within the numerical scheme suggested in this study, and to accumulate a necessary experience for dealing with other problems. In a double-connected region  $\Omega_0$  representing the half-plane  $\Omega \{-\infty < x < \infty, 0 < y < \infty\}$  weakened with an elliptic aperture  $\Gamma$ .

$$\frac{x^2}{p^2} + \frac{(y - y_0)^2}{q^2} = 1 \text{ we consider the boundary-value problem}$$

$$u(x, 0) = 0, u|_T = \psi(x, y) \quad (46)$$

for the Laplace equation.

Let  $\Psi(x, y)$  be the trace on of a profile  $G(x, y; \xi^*, \eta^*)$  of the Green's function of the Dirichlet problem for the half-plane, with the source point  $(\xi^*, \eta^*)$  arbitrarily fixed inside the aperture. This makes  $G(x, y; \xi^*, \eta^*)$  itself, as a function of  $x$  and  $y$ , the exact solution to the problem in (46) in  $\Omega_0$ . The data in Table 1 illustrate the accuracy level attained. They were obtained for the parameters:

$p=2, q=1$ , and  $y_0=3$ . An optimal shape of the fictitious contour  $\Gamma'$  was found as an ellipse centered at  $(0, y_0)$  with the semi-axes  $0.94p$

(x, y)	(0, 2:00)	(0, 1:65)	(0, 1:30)	(0, 0:95)	(0, 0:60)	(0, 0:25)
uappr (x, y)	.42957	.30003	.21258	.14541	.08824	.03602
uexact(x, y)	.42948	.29995	.21251	.14533	.08817	.03593

Table 1: Accuracy level attained for the problem setting in equation 46.

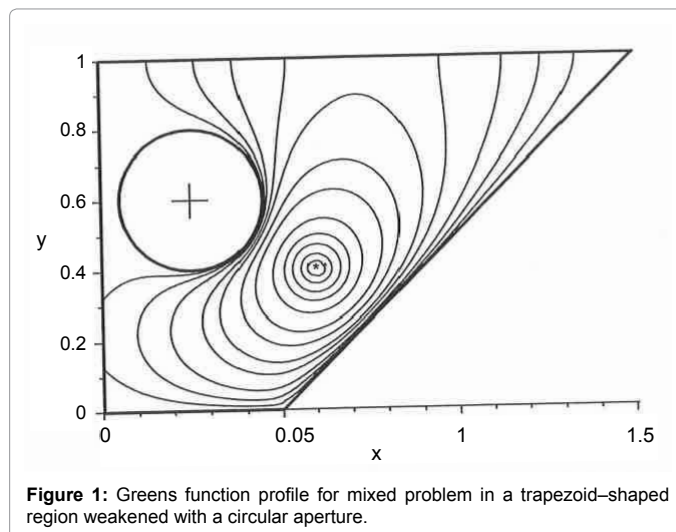


Figure 1: Greens function profile for mixed problem in a trapezoid-shaped region weakened with a circular aperture.

and  $0.93q$ . The standard trapezoid rule, with 24 uniformly distributed on  $\Gamma'$  mesh-points, was used to approximately solve the resolving functional equation.

With an experience gained while dealing with the above sample problem, we go to illustrative examples, and begin with the boundary-value problem

$$u|_{L_1} = 0, \left( \frac{\partial u}{\partial x} - 5u \right)|_{L_2} = 0, \frac{\partial u}{\partial y}|_{L_3} = 0 \quad (47)$$

$$u|_{L_4} = 0, u|_T = 0 \quad (48)$$

stated for the Laplace equation in a double-connected region  $\Omega$  bounded, from outside, with the straight line segments:  $y=0$  (which we refer to as  $L_1$ ),  $x=0$  ( $L_2$ ),  $y=1$  ( $L_3$ ), and  $y=x-0.5$  ( $L_4$ ), whilst from inside it is bounded with the elliptic contour (Figure 1)

$$\frac{(x - x_0)^2}{p^2} + \frac{(y - y_0)^2}{q^2} = 1$$

which is referred to as  $\Gamma$ . So, the region  $\Omega$  might be viewed as a right trapezoid weakened by the elliptic aperture  $\Gamma$ .

We compute the Green's function  $G(x, y, \xi, \eta)$  for the boundary-value problem in (47)-(48) with the aid of the algorithm described in Description of the GF-MFE procedure part. The representation from (26), with the parameter values of  $b=1$  and  $\beta=5$ ; is used in this case as the resolving Green's function  $\tilde{G}(x, y, \xi, \eta)$  in terms of which the function  $G(x, y, \xi, \eta)$  itself is expressed as

$$G(x, y, \xi, \eta) = \tilde{G}(x, y, \xi, \eta) + \int_{L_{4f}} \tilde{G}(x, y, \xi, \eta) \mu_1(\xi, \eta) dL_{4f} \\ + \int_{T_f} \tilde{G}(x, y, \xi, \eta) \mu_2(\xi, \eta) dT_f(\xi, \eta), (x, y) \in \Omega$$

where  $L_{4f}$  and  $\Gamma_f$  represent corresponding fictitious contours. With the above integral representation for  $G(x, y, \xi, \eta)$  the conditions in (48) result subsequently in a system of functional equations in the density functions  $\mu_1(\xi, \eta)$  and  $\mu_2(\xi, \eta)$ .

An issue that makes the problem in (47)-(48) non-trivial for numerical implementations is that the  $L_4$  fragment crosses the pieces  $L_1$  and  $L_3$  of the contour of the semi-infinite strip. But, as our illustrations

will show, the algorithm appears to be capable to successfully overcome such a hurdle.

Profiles of the Green's function  $G(x, y, \xi, \eta)$  computed for a number of problem settings in (47)-(48) are presented in Figures 1, 2, and 3 for a variety of parameters ( $x_0, y_0, p$  and  $q$ ) of the elliptic aperture, and the source point location. The case with a modest size circular aperture and a single source, relatively remote from the exterior boundary of  $\Omega$ , is depicted in Figure 1. The case of a relatively small elliptic aperture, with two sources closely located to the aperture's contour, is presented in Figure 2, and the case of a quite large elliptic hole at an immediate proximity of the exterior boundary is shown in Figure 3. Observing the forenamed, one can conclude that the described method appears efficient for a quite wide range of applications.

Another set of illustrative examples includes a few problems stated in regions having foreign inclusions and weakened with apertures. Potential fields, generated by point sources in such regions, are also computed using the Green's function modification of the method of functional equations. In Figure 4, for example, a profile of  $G(x, y, \xi, \eta)$  is depicted for the half-plane  $y \geq 0$ , having a foreign ( $\lambda=0.01$ ) elliptic inclusion, which in turn is weakened with an eccentric elliptic hole. As to the geometry of the statement, it is forth noting that the hole is located quite far from the material interface line, but the source point is

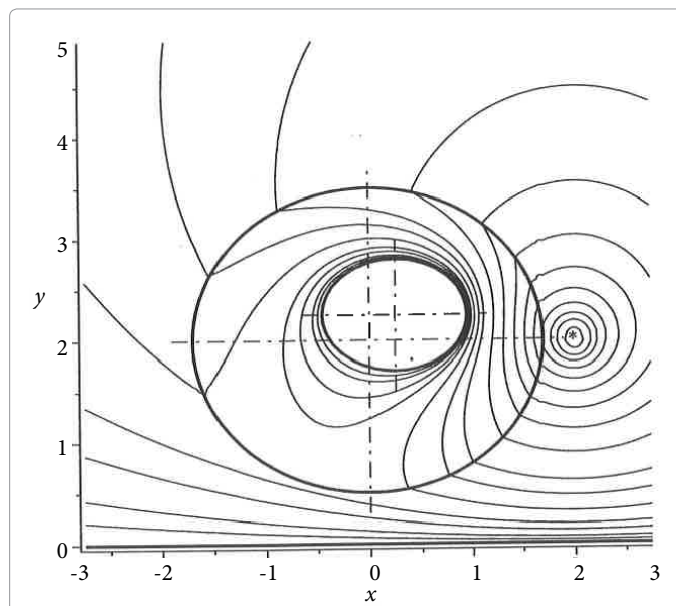


Figure 4: Half-plane hosting an elliptic inclusion weakened with an aperture.

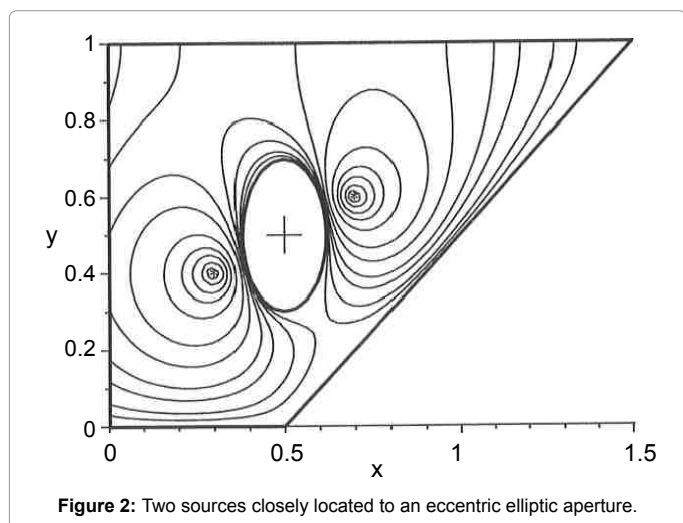


Figure 2: Two sources closely located to an eccentric elliptic aperture.

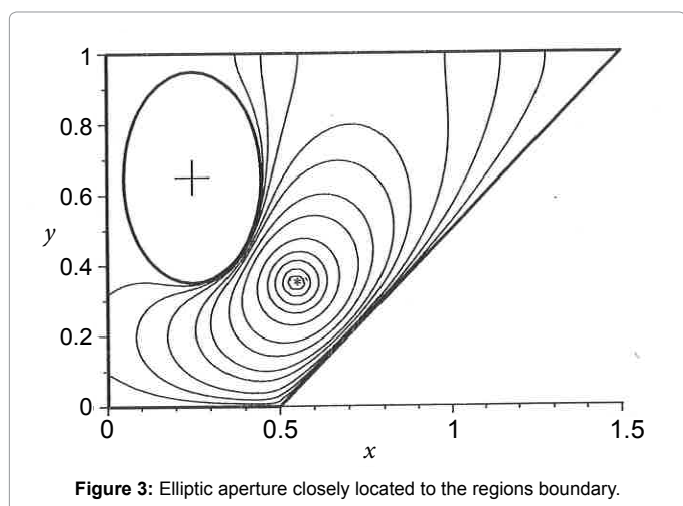


Figure 3: Elliptic aperture closely located to the regions boundary.

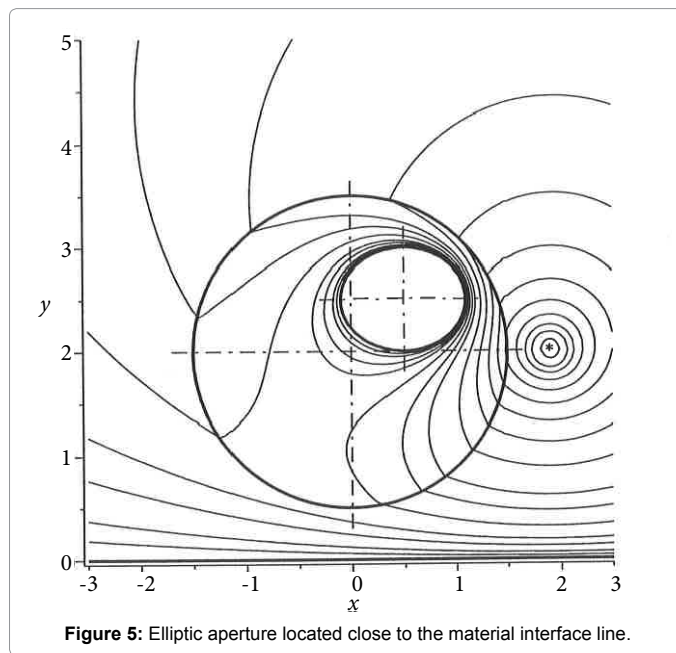


Figure 5: Elliptic aperture located close to the material interface line.

at a relatively close vicinity of that line.

In Figure 5, we present the case that is nearly similar to the previous, except for the location of the hole, which is quite close to the material interface line, but it can be seen that the algorithm still shows a remarkable potential.

In the case presented in Figure 6, the profile of a potential field generated by a point source is depicted for the half-plane  $y \geq 0$  hosting an elliptic inclusion made of a foreign ( $\lambda=0.01$ ) material. The inclusion is weakened with a hole whose contour is a smooth convex closed curve

$$(x - x_h)^4 + (y - y_h)^4 = R^4$$

which sometimes is referred to as a fat circle. It is important to note that both the source point and the hole's contour are rather remote

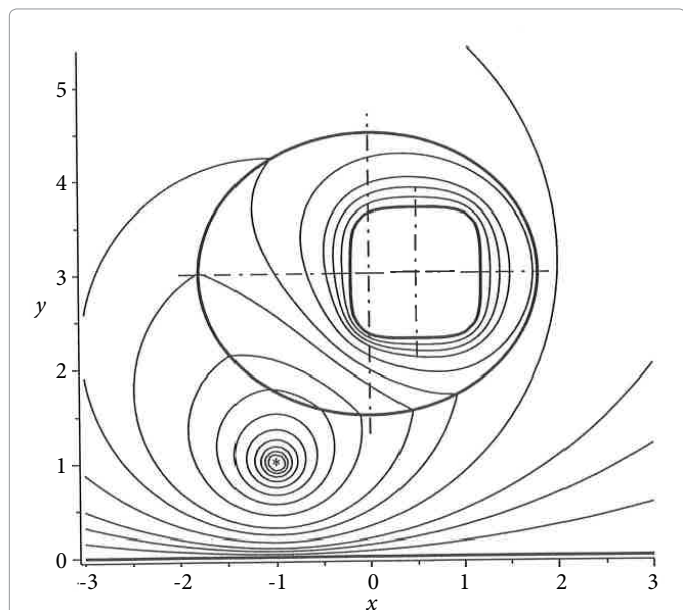


Figure 6: Half- plane hosting an inclusion weakened with a fat circle aperture.

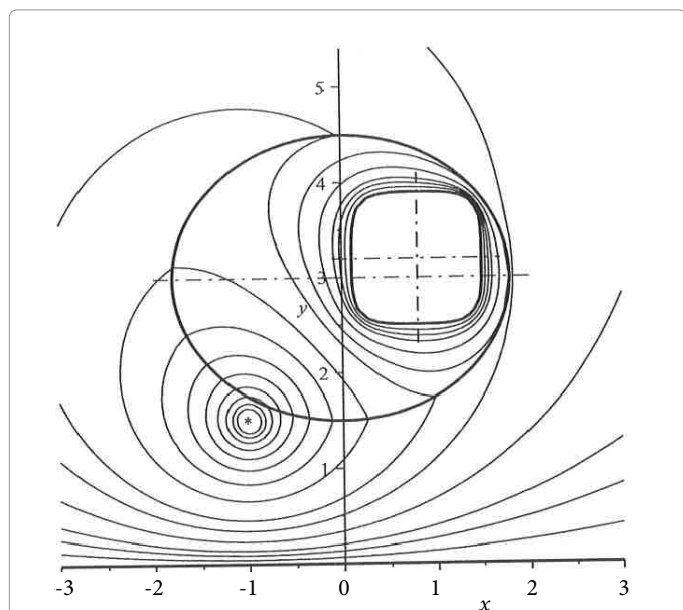


Figure 7: Source and aperture located close to the material interface line.

from the material interface line. In Figure 7, in contrast, both of them are relatively close to the interface line, but this complication does not affect our algorithm.

A case of the semi-infinite strip  $\{Re(z)>0, 0<Im(z)<1\}$ , hosting an elliptic inclusion made of a foreign ( $\lambda=0.1$ ) material and weakened with an elliptic aperture, is shown in Figure 8. The boundary conditions are imposed on the segments  $y=0$  ( $L_1$ ),  $x=0$  ( $L_2$ ), and  $y=1$  ( $L_3$ ) of the semi-strip's boundary as:

$$u|_{L_1} = 0, \left( \frac{\partial u}{\partial x} - 0.5u \right) \Big|_{L_2} = 0, \frac{\partial u}{\partial y} \Big|_{L_3} = 0$$

Thus, from the presented illustrations, it follows that the location

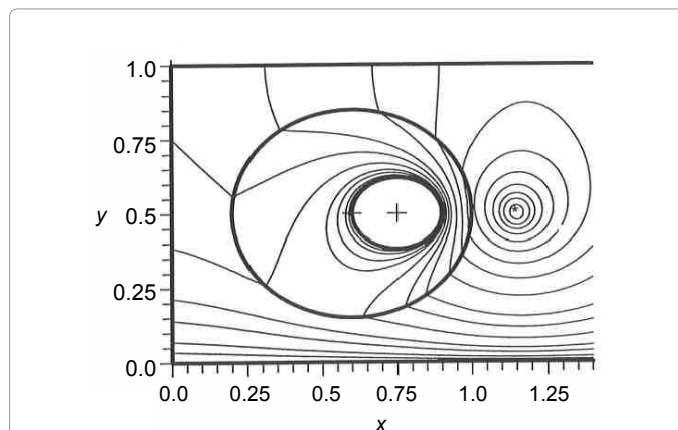


Figure 8: Green's function profile for mixed problem in a semi-strip hosting an inclusion weakened with an aperture.

of a point source as well as the location and the shape of an inclusion or an aperture have not been decisive factors for the proposed algorithm.

### Concluding Remarks

The data presented and discussed in this study build up a confidence in the GF-MFE applied to a broad variety of boundary-value problems set up in multiply-connected regions for elliptic partial differential equations with piecewise constant coefficients. The most notable feature, that makes the GF-MFE efficient computationally, is the use of resolving Green's functions or matrices of Green's type. This significantly reduces the required computer time compared to other traditional approaches of the method of boundary integral equations, because some of the boundary conditions in the problem are taken care of prior to the actual numerical work. Note, however, that some computer-friendly forms of the resolving Green's functions are required.

### References

- Smirnov VI (1964) A Course of Higher Mathematics: Integral equations and partial differential equations. Pergamon Press, Oxford New York 4.
- Kupradze VD, Aleksidze MA (1964) The method of functional equations for the approximate solution of certain boundary-value problems, USSR Computational Mathematics and Mathematical Physics 4: 683-715.
- Bogomolny A (1985) Fundamental solutions method for elliptic boundary-value problems. SIAM J Numerical Analysis 22: 644-669.
- Melnikov YA (1977) Some applications of the Green's function method in mechanics, International Journal of Solids and Structures 13: 1045-1058.
- Melnikov YA (1998) Green's function formalism extended to systems of mechanical differential equation posed on graphs. Journal of Engineering Mathematics 34: 369-386.
- Melnikov YA (1999) Influence Functions and Matrices, Marcel Dekker, New York Basel.
- Melnikov YA, Melnikov MY (2006) Computability of series representations for Green's functions in a rectangle. Engineering Analysis with Boundary Elements 30:774-780.
- Melnikov YA (2010) Efficient representations of Green's functions for some elliptic equations with piecewise-constant coefficients. Central European Journal of Mathematics 8: 53-72.
- Korn GA, Korn TM (1968) Mathematical Handbook for Scientists and Engineers, McGraw Hill, New York.
- Pinsky MA (1998) Partial Differential Equations and Boundary-Value Problems with Applications, McGraw Hills Boston.